Chinese Chemical Letters 37 (2026) 111975

Contents lists available at ScienceDirect

Chinese Chemical Letters

journal homepage: www.elsevier.com/locate/cclet

Recyclable construction of chiral hydrogen-bonded frameworks *via* inducer-modulated spontaneous resolution for enantioselective sensing

Bin Zhao[a], Wenyue Cui[a], Wenhao Huang[a], Zongsu Han[a], Zhonghang Chen[a], Peng Cheng[a,b], Wei Shi[a,*]

[a] *Frontiers Science Center for New Organic Matter, State Key Laboratory of Advanced Chemical Power Sources, and Department of Chemistry, College of Chemistry, Nankai University, Tianjin 300071, China*
[b] *Haihe Laboratory of Sustainable Chemical Transformations, Tianjin 300192, China*

ARTICLE INFO

Article history:
Received 24 June 2025
Revised 13 October 2025
Accepted 15 October 2025
Available online 16 October 2025

Keywords:
Spontaneous resolution
Chiral induction
Inducer modulation
Hydrogen-bonded framework
Enantioselective sensing

ABSTRACT

Spontaneous resolution is a way for constructing chiral compounds from achiral modules, but the products are usually stochastic, which is unsuitable for enantioselective applications. Herein, a pair of chiral hydrogen-bonded frameworks assembled from achiral modules was reported. By introducing reusable chiral inducers, enantiomerically enriched NKU-777-*xD*/*xL* were obtained and exhibited superior enantioselective sensing performance. Notably, the amount of chiral inducer shows a positive correlation with the enantioselective sensing function, reflecting the degree of enantiomeric excess of NKU-777-*xD*/*xL*. Molecular-level mechanism studies reveal that competitive absorption governs the sensing functions of NKU-777-*xD*/*xL*, and the enantioselectivity is due to the enantioselective interactions of the hydrogen-bonded frameworks with targeting chiral molecules. This work not only provides a facile way to synthesize enantiomerically enriched chiral hydrogen-bonded frameworks from achiral modules using reusable chiral inducer but also gains insights into the inducer-controlled enantiomerically enriched chiral compounds for enantioselective applications.

© 2026 Published by Elsevier B.V. on behalf of Chinese Chemical Society and Institute of Materia Medica, Chinese Academy of Medical Sciences.

Enantiomers, typically possessing highly similar structures and properties, may exhibit different or even opposite biological activities [1–6]. The construction of advanced chiral sensing materials is crucial for monitoring the enantiomers used in pharmaceutical industry and public health; however, the synthesis of chiral compounds is generally constrained by the complex crystallization process in low-symmetry space groups. Spontaneous resolution is a unique crystallization process based on the symmetry breaking of achiral modules, offering a key approach for constructing chiral compounds. In general, it is highly challenging to achieve enantiomerically enriched products from spontaneous resolution for enantioselective applications [7–15]. Chiral induction is a promising strategy for achieving enantiomerically enriched chiral products *via* spontaneous resolution, based on the disruption to the symmetry of the racemic system by suitable inducer [16–22]. However, due to the complicated coordination and crystallization processes, the mechanism governing chiral induction for spontaneous resolution has not yet been well elucidated [23].

Hydrogen-bonded framework based on coordination-unit is a type of highly ordered framework compounds, which is constructed by multiple weak interactions among coordination units [24–31]. These compounds combine the advantages of inorganic and organic modules, which typically exhibit dynamic adjustability and flexibility, and possess promising applications in catalysis [32–35], adsorption and separation [36–41], circularly polarized luminescence [42–44], and molecular recognition [45–49]. Generally, besides direct synthesis [50,51] and post-synthesis modification with chiral ligands [52], spontaneous resolution [53] has been used to construct chiral hydrogen-bonded frameworks; however, due to the inherent directionality and weak interactions of hydrogen bonds, it is highly unpredictable to synthesize such chiral framework compounds, especially for those that are enantiomerically enriched.

Herein, we report the rational synthesis of chiral coordination-chain-based hydrogen-bonded frameworks NKU-777-*xD*/*xL* ($x = 0.1$, 0.2, 0.3, 0.4, 0.5, 0.6, 0.7) through spontaneous resolution *via* introducing chiral inducer D/L-mandelic acid (D/L-MA). Single

* Corresponding author.
E-mail address: shiwei@nankai.edu.cn (W. Shi).

https://doi.org/10.1016/j.cclet.2025.111975
1001-8417/© 2026 Published by Elsevier B.V. on behalf of Chinese Chemical Society and Institute of Materia Medica, Chinese Academy of Medical Sciences.

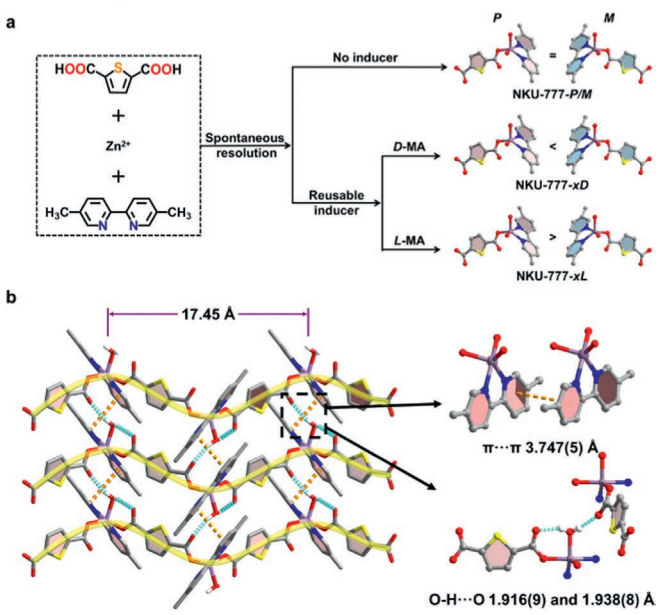


Fig. 1. Synthesis and structure analysis. (a) The synthesis of racemic products of NKU-777-*P*/*M* and enantiomerically enriched NKU-777-*xD*/*xL*. (b) The coordination-chain-based hydrogen-bonded framework (left) and two types of weak interactions (right). Atom code: Zn, light purple; S, yellow; N, blue; C, grey; O, red; H, white.

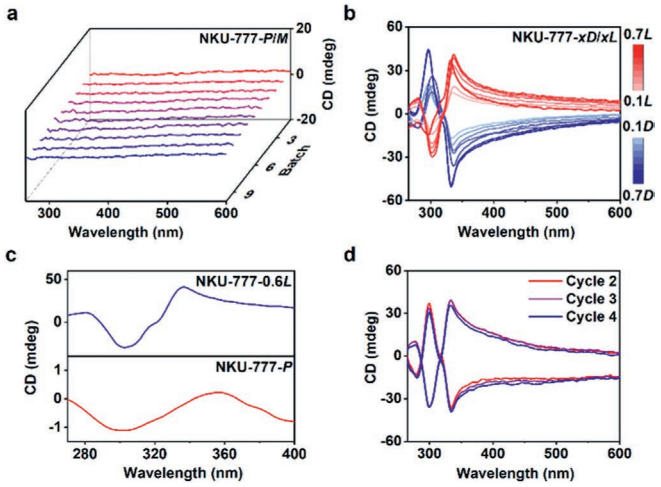


Fig. 2. CD spectra of NKU-777. (a) 10 batches of NKU-777-*P*/*M* synthesized without chiral inducer. (b) NKU-777-*xD* (blue) and NKU-777-*xL*(red) synthesized by introducing different amounts of D/L-MA. (c) NKU-777–0.6*L* and NKU-777-*P*. (d) NKU-777–0.6*D*/0.6*L* synthesized using reusable D/L-MA.

crystals of [Zn(tpdc)(Me_2dpy)(H_2O)] (NKU-777-*P*/*M*, H_2tpdc = 2,5-thiophenedicarboxylic acid, Me_2dpy = 5,5′-dimethyl-2,2′-dipyridyl) were obtained for structural analysis. NKU-777-*xD*/*xL* exhibited enantioselective sensing functions of enantiomers. Notably, the positive correlation between inducer concentration and enantioselective sensing result were revealed, indicating that the symmetry breaking process is inducer concentration-dependent. Moreover, the inducer can be reused. Mechanism studies show that competitive absorption governs the sensing property, and enantioselectivity can be attributed to the difference in binding affinities between NKU-777-*xD*/*xL* and chiral analytes.

The racemic single crystals of NKU-777-*P*/*M* were synthesized by solvothermal reaction of zinc nitrate hexahydrate, H_2tpdc and Me_2dpy (Fig. 1a). NKU-777-*P*/*M* crystallize in the monoclinic chiral space group $P2_1$. NKU-777-*P* was selected as the representative for structure description. The asymmetric unit of NKU-777-*P* consists of one Zn^{2+} ion, one $tpdc^{2-}$, one Me_2dpy, and one water molecule. Zn^{2+} ion is five-coordinated by two O atoms from two $tpdc^{2-}$, two N atoms from Me_2dpy, and one water molecule (Fig. S1a in Supporting information). The Zn-O bond lengths are in the range of 1.964(2)-2.055(4) Å, and the Zn-N bond lengths are 2.103(9) and 2.154(4) Å. Each $tpdc^{2-}$ coordinates to two Zn^{2+} ions which are bidentate chelated by Me_2dpy, forming a chain with 2_1 helix along the *b*-axis with a helical pitch of 17.45 Å (Fig. 1b). The adjacent chains are linked by multiple O–H···O hydrogen bonding interactions (1.938(8) and 1.916(9) Å) between the coordinated water molecules and carboxyl group of $tpdc^{2-}$, as well as $\pi\cdots\pi$ interaction (3.747(5) Å) between adjacent Me_2dpy molecules, producing a two-dimensional supramolecular framework (Figs. S1b and c in Supporting information).

The phase purities of NKU-777-*P*/*M* are validated by powder X-ray diffraction (PXRD) (Fig. S2 in Supporting information). The Fourier transform infrared (FTIR) spectra of NKU-777-*P*/*M* displayed blue shifts of the carbonyl group and the pyridine ring, indicating the coordination with Zn^{2+} ions (Fig. S3 in Supporting information). Thermogravimetric analysis indicates that there is no significant weight loss for NKU-777-*P*/*M* from 40 °C to 110 °C, and the weight loss from 110 °C to 180 °C is attributed to the loss of one coordinated water molecule (Fig. S4 in Supporting information). The absolute configuration of the single crystal of NKU-777-*P*/*M* was confirmed by the Flack parameter (~0) derived from single crystal X-ray diffraction analysis (Table S1 in Supporting information) [54,55].

To investigate the spontaneous resolution result of NKU-777-*P*/*M*, 20 randomly selected single crystals were subjected to single crystal X-ray diffraction analysis. The results show that 9 crystals belong to NKU-777-*P*, while 11 crystals belong to NKU-777-*M* (Table S2 in Supporting information). Additionally, circular dichroism (CD) tests were conducted on 10 different batches of the samples, and no significant Cotton effect was detected (Fig. 2a). These results indicate that spontaneous resolution yields a mixture composed of enantiomerically pure NKU-777-*P* and NKU-777-*M* crystals. In addition, the distinct optical activities of the enantiomers were observed under a polarizing microscope, demonstrating the successful resolution of chirality in NKU-777-*P*/*M* (Fig. S5 in Supporting information).

To obtain enantiomerically enriched NKU-777-*P*/*M*, eight different L-amino acids, were used as chiral inducer. The CD spectra revealed that L-MA has a superior chiral induction capability compared to others (Fig. S6 in Supporting information), and hence D/L-MA was employed for further experiments. NKU-777-*xD* and NKU-777-*xL* were synthesized by introducing *x* (*x* = 0.1, 0.2, 0.3, 0.4, 0.5, 0.6, 0.7) mmol of inducer *via* a one-pot method, and no product was obtained when *x* exceeded 0.7. The CD spectra of NKU-777-*xD*/*xL* showed significant Cotton effects at 300 and 342 nm, corresponding to the absorption of $tpdc^{2-}$ and Me_2dpy, respectively (Fig. 2b and Fig. S7 in Supporting information), indicating that D/L-MA is an effective chiral inducer for achieving enantiomerically enriched NKU-777-*P*/*M*. At the same time, to elucidate the correlation between the products induced by D/L-MA and the corresponding NKU-777-*P* and NKU-777-*M*, the crystals of NKU-777-*P* screened by single crystal X-ray diffraction were subjected to CD test. The result revealed that in NKU-777-*xL*, NKU-777-*P* emerged as the predominant excess species (Fig. 2c).

To confirm the chiral origin of NKU-777-*xD*/*xL*, a series of characterizations were performed, including PXRD (Figs. S8 and S9 in Supporting information), FTIR (Figs. S10 and S11 in Supporting information), and ^{1}H nuclear magnetic resonance (NMR) spectra (Figs. S12-S14 in Supporting information). PXRD and FTIR spectra of NKU-777-*xD*/*xL* showed no significant alterations upon adding

the inducer, suggesting that the addition of D/L-MA did not result in any structural transformation of NKU-777-*P*/*M* or the formation of other crystalline phases. ^{1}H NMR spectra indicate that there are no characteristic chemical shifts of D/L-MA in NKU-777-*xD*/*xL*, suggesting that D/L-MA is absent in the products. These findings collectively confirm that the observed Cotton effects are attributed to the supramolecular frameworks but not from D/L-MA.

In addition, after the product is separated from the mother solution, the achiral building blocks were added, and the products were subjected to PXRD (Fig. S15 in Supporting information), FTIR (Fig. S16 in Supporting information), and CD characterizations (Fig. 2d). The results indicate that even without adding extra chiral inducer, NKU-777–0.6*D* and NKU-777–0.6*L* can still be obtained, indicating the reusability of D/L-MA in the solution.

To investigate the sensing application of NKU-777-*xD*/*xL*, the photophysical properties were tested. The photoluminescence (PL) spectra of NKU-777-*P*/*M* were measured in the ethanol dispersion (Fig. S17 in Supporting information). An emission peak at 342 nm was observed excited at 315 nm. The cyclic luminescence experiments over 65 cycles within a 10-min period revealed that NKU-777-*P*/*M*, NKU-777–0.6*D*, and NKU-777–0.6*L* possess high luminescence stabilities (Figs. S18-S20 in Supporting information). The quantum yield of NKU-777-*P*/*M* is 37.76% (Fig. S21 in Supporting information), demonstrating the excellent emission efficiency.

The enantiomers of (1*S*,2*S*)-(+)-1,2-diphenylethylenediamine (*S*-DPEAN) and (1*R*,2*R*)-(+)-1,2-diphenylethylenediamine (*R*-DPEAN) were selected to test the enantioselective sensing properties of NKU-777-*xD*/*xL*, where *S*/*R*-DPEAN and their derivatives being crucial in asymmetric synthesis [56–59]. The sensing capabilities of NKU-777-*xD*/*xL* were firstly evaluated through their response to single-component enantiomer (Figs. S22-S25 in Supporting information). The emission intensities of NKU-777-*xD*/*xL* at 342 nm diminish progressively upon introducing *S*/*R*-DPEAN. Furthermore, the quenching efficiencies of *S*/*R*-DPEAN exhibit distinct tendencies for NKU-777-*xD*/*xL*, which were obtained by fitting the luminescence titration data based on exponential nonlinear Stern-Volmer (S-V) equation (Figs. S26 and S27 in Supporting information) and linear S-V equation (Figs. S28 and S29 in Supporting information) [60–64], respectively (Tables S3-S6 in Supporting information). Notably, the $K_{SV\text{-}S}$ values of NKU-777-*xD* to *S*-DPEAN consistently exceeds that of its enantiomer. For comparison, for NKU-777-*xL*, $K_{SV\text{-}R}$ is higher than $K_{SV\text{-}S}$. Importantly, the ratio of $K_{SV\text{-}S}$ and $K_{SV\text{-}R}$ steadily increases as the molar quantity of D/L-MA increase (Fig. 3a), to reach the value of 2.07 at $x = 0.6$. When x is increased to 0.7, no further change in K_{SV} was observed. This result indicates that NKU-777-*xD*/*xL* exhibits different enantioselective sensing performance towards *S*/*R*-DPEAN, and this difference arises from varied ratios of enantiomers of enantiomerically enriched NKU-777-*xD*/*xL*.

The enantioselective sensing properties of NKU-777-*P*/*M* and NKU-777-*xD*/*xL* towards *S*/*R*-DPEAN enantiomer mixtures were further studied (Fig. 3b, Figs. S30-S38 and Table S7 in Supporting information). NKU-777-*P*/*M* displayed almost no selective sensing performance. However, NKU-777–0.3*D* and NKU-777–0.6*D* exhibited distinct emission responses to varied enantiomeric excess (*ee*) values. NKU-777–0.6*D* demonstrated better sensitivity compared to NKU-777–0.3*D*.

The enantioselective sensing properties of the cyclic NKU-777–0.6*D* and NKU-777–0.6*L* were investigated (Figs. S39 and S40 in Supporting information). The quenching efficiency was obtained by fitting luminescence titration data using exponential nonlinear S-V equation (Figs. S41 and S42 in Supporting information) and linear S-V equation (Figs. S43 and S44 in Supporting information), respectively (Tables S8-S11 in Supporting information). The K_{SV} ratio of the products showed no significant changes during four cycles (Figs. 3c and d), with relative standard deviations within 5%, demonstrating the reusability of the D/L-MA.

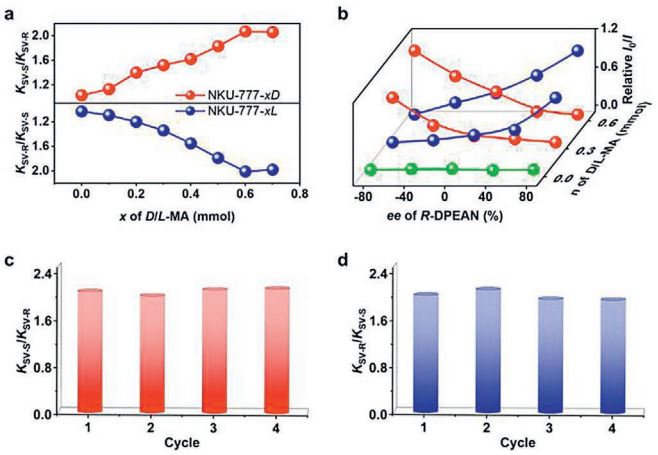


Fig. 3. Enantioselective sensing results of NKU-777-*xD*/*xL*. (a) The relationship between K_{SV} ratios and D/L-MA molar content. (b) Sensing performance of NKU-777-*P*/*M* (green), NKU-777-*xD* (red) and NKU-777-*xL* (blue) towards *S*/*R*-DPEAN with different *ee* values. (c) The K_{SV} ratio of NKU-777–0.6*D* synthesized using reusable D-MA. (d) The K_{SV} ratios of NKU-777–0.6*L* synthesized using reusable L-MA.

The sensing mechanism was studied through a series of characterizations, including PXRD, PL spectrum, fluorescence lifetime and ultraviolet-visible (UV–vis) spectrum and molecular energy level calculation. PXRD patterns of NKU-777-*xD*/*xL* before and after sensing were tested (Figs. S45 and S46 in Supporting information). There is no significant alteration in the PXRD patterns of the samples, indicating that the sensing is not attributable to the structural transformation. The luminescence emission spectrum of NKU-777-*P*/*M* and the ultraviolet absorption spectrum of *S*/*R*-DPEAN have almost no overlap, demonstrating that there is no fluorescence resonance energy transfer (FRET) between NKU-777-*P*/*M* and *S*/*R*-DPEAN (Fig. 4a and Fig. S47 in Supporting information) [65–67]. The lowest unoccupied molecular orbital (LUMO) of H_2tpdc and Me_2dpy is lower than that of *S*/*R*-DPEAN (Fig. 4b), indicating the response of NKU-777-*P*/*M* to *S*/*R*-DPEAN does not involve the photoinduced electron transfer (PET) mechanism [68–70]. The fluorescence lifetime did not change significantly before and after titration, confirming that the interaction of NKU-777-*P*/*M* and *S*/*R*-DPEAN is static (Figs. S48-S51, Tables S12 and S13 in Supporting information) [71–73]. UV–vis spectra of NKU-777-*P*/*M* and *S*/*R*-DPEAN indicate an overlap within the 200–400 nm wavelength range, demonstrating that competitive absorption (CA) is the underlying mechanism for sensing functions (Fig. 4c) [74,75].

To further elucidate the enantioselective sensing mechanism, the CD titration experiment of NKU-777–0.6*D* was performed toward *S*/*R*-DPEAN (Fig. 4d, Fig. S52 and Table S14 in Supporting information). The decreased efficiency of the absorption peaks of NKU-777–0.6*D* depends on the strength of the electrostatic interactions between the host and guest molecules. *S*-DPEAN has a higher quenching rate for NKU-777–0.6*D* compared to that of *R*-DPEAN, indicating that NKU-777–0.6*D* interacts more strongly toward *S*-DPEAN due to the structural compatibility between NKU-777–0.6*D* and *S*-DPEAN, resulting in a more efficient quenching result (Fig. 4e).

In summary, we report a facile strategy for assembling chiral supramolecular frameworks from achiral building blocks for enantioselective sensing. Enantiomerically enriched NKU-777-*xD*/*xL* are synthesized through a chirality-induced spontaneous resolution process with reusable chiral inducer. The enantioselective sensing properties of NKU-777-*xD*/*xL* have been studied in details, revealing the positive correlation between inducer concentration and

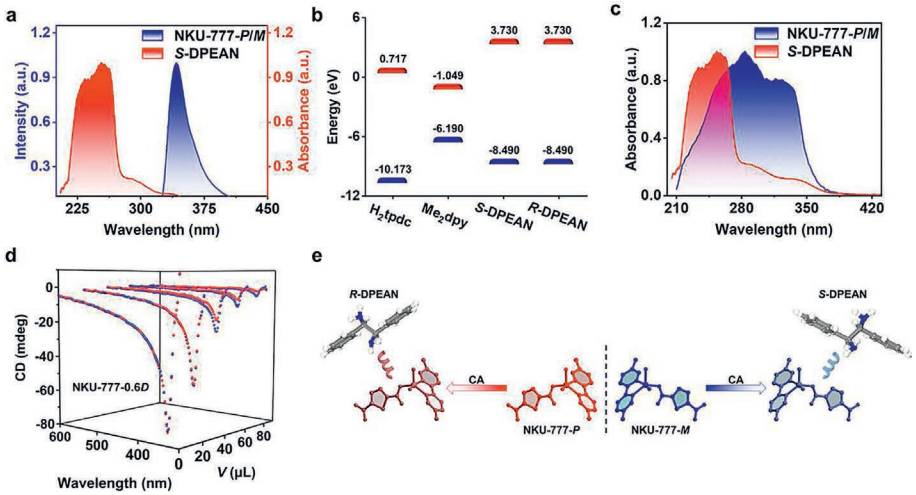


Fig. 4. The sensing mechanism of NKU-777-*xD*/*xL*. (a) The luminescence emission spectrum of NKU-777-*P*/*M* synthesized without inducer and the UV–vis spectrum of *S*-DPEAN. (b) Energy levels of H_2tpdc, Me_2dpy, *S*-DPEAN, and *R*-DPEAN (red: LUMO, blue: HOMO). (c) UV–vis spectra of NKU-777-*P*/*M* and *S*-DPEAN. (d) CD titrations of NKU-777–0.6*D* towards *S*-DPEAN (red) and *R*-DPEAN (blue). (e) The enantioselective sensing mechanism of NKU-777-*xD*/*xL* toward the analytes.

enantioselective sensing properties. Importantly, NKU-777-*xD*/*xL* demonstrated the determination of *ee* values of targeting racemic mixtures. The sensing mechanism is mainly based on the competitive absorption of the excited energy between the framework and the enantiomers, while the enantioselectivity is attributed to the enantioselective interactions of the framework and the enantiomers. This work not only provides a facile and cyclic synthetic way for spontaneous resolution, but also reveals the concentration effect of chiral induction in the cost-effective construction of chiral sensing materials from achiral building blocks, which could be useful for spontaneous resolution of tailored chiral products.

Declaration of competing interest

The authors declare that they have no known competing financial interests or personal relationships that could have appeared to influence the work reported in this paper.

CRediT authorship contribution statement

Bin Zhao: Writing – original draft, Formal analysis, Data curation. **Wenyue Cui:** Formal analysis. **Wenhao Huang:** Formal analysis. **Zongsu Han:** Formal analysis. **Zhonghang Chen:** Formal analysis. **Peng Cheng:** Supervision. **Wei Shi:** Writing – review & editing, Supervision.

Acknowledgments

This work was supported by the National Key Research and Development Program of China (No. 2024YFE0211600), the National Natural Science Foundation of China (Nos. 22261132509, 22471130, 22435002 and 22121005) and the “111 Center” (No. B25010), and the Natural Science Foundation of Tianjin (No. 22JCYBJC00740).

Supplementary materials

Supplementary material associated with this article can be found, in the online version, at doi:10.1016/j.cclet.2025.111975.

References

[1] X. Zhou, Z. Wang, S. Li, et al., Science 383 (2024) 612–618.
[2] I. Popov, Science 372 (2021) 688.
[3] D. Glavin, A. Burton, J. Elsila, J. Aponte, J. Dworkin, Chem. Rev. 120 (2020) 4660–4689.
[4] T. Kirby, Lancet 402 (2023) 2182.
[5] H. Furihata, S. Yamanaka, T. Honda, et al., Nat. Commun. 11 (2020) 4578.
[6] J. Cheng, J. Jiang, B. He, et al., Sci. Transl. Med. 15 (2023) e6543.
[7] T. Buhse, J.M. Cruz, M. Noble-Terán, et al., J. Micheau, Chem. Rev. 121 (2021) 2147–2229.
[8] F. García, R. Gómez, L. Sánchez, Chem. Soc. Rev. 52 (2023) 7524–7548.
[9] T. Ezuhara, K. Endo, Y. Aoyama, J. Am. Chem. Soc. 121 (1999) 3279–3283.
[10] F. Esteve, B. Altava, E. Garcla, S. Luis, J. Lehn. Chem 8 (2022) 2023–2042.
[11] G. Zhang, L. Wang, J. Wang, et al., Nat. Commun. 14 (2023) 3046.
[12] M. Yu, C. Liu, Y. Zhao, et al., Angew. Chem. Int. Ed. 61 (2022) e202201590.
[13] R. Viswanathan, J. Zasadzinski, D. Schwartz, J. Am. Chem. Soc. 144 (2022) 1342–1350.
[14] D. Wu, K. Zhou, J. Tian, et al., Angew. Chem. Int. Ed. 60 (2021) 3087–3094.
[15] Y. Zuo, X. Liu, E. Fu, S. Zhang, Angew. Chem. Int. Ed. 62 (2023) e202217225.
[16] A. Kanj, J. Bürck, N. Vankova, et al., J. Am. Chem. Soc. 143 (2021) 7059–7068.
[17] T. Zhuang, Y. Li, X. Gao, et al., Nat. Nanotechnol. 15 (2020) 192–197.
[18] G. Wang, A. Qu, M. Sun, J. Xu, H. Kuang, Acc. Mater. Res. 5 (2024) 1221–1236.
[19] A. Mondal, M. Preuss, M. Ślęczkowski, et al., J. Am. Chem. Soc. 143 (2021) 7189–7195.
[20] M. Ślęczkowski, M. Mabesoone, P. Ślęczkowski, A. Palmans, E. Meijer, Nat. Chem. 13 (2021) 200–207.
[21] A. Hassanfiroozi, Y. Lu, P. Wu, Adv. Mater. 36 (2024) 2410568.
[22] R. Li, Q. Deng, L. Han, et al., Nat. Commun. 15 (2024) 10130.
[23] W. Gong, Z. Chen, J. Dong, Y. Liu, Y. Cui, Chem. Rev. 122 (2022) 9078–9144.
[24] Y. Xie, X. Ding, J. Wang, G. Ye, Angew. Chem. Int. Ed. 62 (2023) e202313951.
[25] R. Chen, S. Wang, Y. Liu, J. Zhang, W. Fang, J. Am. Chem. Soc. 146 (2024) 7524–7532.
[26] Z. Han, R. Zhang, J. Jiang, et al., J. Am. Chem. Soc. 145 (2023) 10149–10158.
[27] Y. Liu, L. Wang, L. Zhao, et al., Chem. Soc. Rev. 53 (2024) 1592–1623.
[28] Y. Hamada, S. Ogi, S. Yamaguchi, Angew. Chem. Int. Ed. 63 (2024) e202409657.
[29] Z. Zhai, T. Hou, Y. Xu, et al., Chem. Eur. J. 31 (2025) e202403699.
[30] J. Liu, J. Jiang, Q. Zhou, et al., eScience 3 (2023) 100094.
[31] Z. Han, K. Wang, M. Wang, et al., Chem 9 (2023) 2561–2572.
[32] J. Chen, Y. Huang, J. Yang, et al., J. Am. Chem. Soc. 146 (2024) 32738–32747.
[33] Z. Li, Y. Xiao, C. Jiang, et al., Natl. Sci. Rev. 11 (2024) neae332.
[34] Z. Zhang, X. Hu, S. Qiu, et al., J. Am. Chem. Soc. 146 (2024) 11328–11341.
[35] R. Chen, A. Hammoud, P. Aoun, et al., Nat. Commun. 15 (2024) 4116.
[36] B. Zhao, L. Yuan, Y. Wang, T. Duan, W. Shi, ACS Appl. Mater. Interfaces 13 (2021) 16300–16308.
[37] L. He, Y. Li, L. Li, et al., Angew. Chem. Int. Ed. 63 (2024) e202418917.
[38] Y. Liu, H. Wu, L. Guo, et al., Angew. Chem. Int. Ed. 61 (2022) e202117609.
[39] P. Li, Y. He, J. Guang, et al., J. Am. Chem. Soc. 136 (2014) 547–549.
[40] X. Song, Y. Wang, C. Wang, et al., J. Am. Chem. Soc. 146 (2024) 627–634.
[41] Z. Chen, L. Zhang, H. Wu, et al., Chem. Sci. 15 (2024) 13191–13200.
[42] X. Tang, H. Jiang, Y. Si, et al., Chem 7 (2021) 2771–2786.
[43] X. Yang, Y.X. Zheng, H. Kuang, et al., CCS Chem. 5 (2023) 2760–2789.
[44] X. Lin, G. Yang, M. Liu, ACS Appl. Mater. Interfaces 15 (2023) 19741–19749.
[45] S. Wang, J. Liu, S. Feng, et al., Angew. Chem. Int. Ed. 63 (2024) e202400742.
[46] Y. Li, H. Chen, J. Huang, et al., J. Am. Chem. Soc. 146 (2024) 19425–19433.
[47] C. Wang, X. Song, Y. Wang, et al., Angew. Chem. Int. Ed. 62 (2023) e202311482.
[48] C. Deng, X. Liu, Z. Wang, W. Lin, Inorg. Chem. 64 (2025) 2583–2589.
[49] X. Zhao, E. Nguyen, A. Hong, P. Feng, X. Bu, Angew. Chem. Int. Ed. 57 (2018) 7101–7105.
[50] D. Kundu, N. Rio, J. Crassous, Acc. Chem. Res. 57 (2024) 2941–2952.
[51] C. Sato, S. Dekura, H. Sato, et al., J. Am. Chem. Soc. 146 (2024) 22699–22710.
[52] Z. Han, M. Wang, K. Wang, P. Cheng, W. Shi, Chem. Eur. J. 29 (2023) e202301892.

[53] D. Luo, X. Wang, C. Yang, X. Zhou, D. Li, J. Am. Chem. Soc. 140 (2018) 118–121.
[54] S. Parsons, H. Flack, T. Wagner, Acta Crystallogr. Sect. B. 69 (2013) 249–259.
[55] R. Dubey, K. Yan, T. Kikuchi, et al., Angew. Chem. Int. Ed. 60 (2021) 11809–11813.
[56] W. Li, T. Wagener, L. Hellmann, C. Daniliuc, et al., J. Am. Chem. Soc. 142 (2020) 7100–7107.
[57] J. Shim, J. Lee, H. Kim, D. Ha, Catalysts 12 (2022) 435.
[58] J. Chen, M. Xu, J. Zhang, et al., ACS Catal. 10 (2020) 3556–3563.
[59] J. Coverdale, I. Canelón, C. Cano, et al., Nat. Chem. 10 (2018) 347–354.
[60] Z. Chen, Y. Lu, L. Wang, et al., J. Am. Chem. Soc. 145 (2023) 260–267.
[61] Y. Zhao, H. Zeng, X. Zhu, W. Lu, D. Li, Chem. Soc. Rev. 50 (2021) 4484–4513.
[62] M. Wang, Z. Han, K. Wang, et al., Angew. Chem. Int. Ed. 63 (2024) e202318722.
[63] Z. Chen, P. Fang, J. Li, et al., Natl. Sci. Rev. 11 (2024) neae342.
[64] Z. Han, K. Wang, Y. Guo, et al., Nat. Commun. 10 (2019) 5117.
[65] C. Xu, J. Xu, H. Tang, et al., Nature 617 (2023) 798–806.
[66] B. Fang, Y. Shen, B. Peng, et al., Angew. Chem. Int. Ed. 61 (2022) e202207188.
[67] O. Sikimić, A. Stiel, M. Kolb, et al., Nature 592 (2021) 768–772.
[68] X. Xu, I. Sahalianov, H. Sun, et al., Angew. Chem. Int. Ed. 64 (2024) e202422856.
[69] J. McCusker, Science 363 (2019) 484–488.
[70] Z. Han, K. Wang, M. Wang, W. Shi, Acc. Chem. Res. 58 (2025) 625–634.
[71] C. Zanetti, L. Li, R. Gaspar, et al., Sensors 24 (2024) 267.
[72] V.Coropceanu Abroshan, J. Brédas, Adv. Funct. Mater. 30 (2020) 2002916.
[73] O. Millington, S. Montanaro, A. Sharma, et al., J. Am. Chem. Soc. 146 (2024) 29664–29674.
[74] Z. Han, T. Sun, R. Liang, et al., J. Am. Chem. Soc. 146 (2024) 15446–15452.
[75] H. Min, Z. Han, T. Sun, et al., Sci. China Chem. 66 (2023) 3511–3517.